The Plant Cell, Vol. 7, 259–270, March 1995 © 1995 American Society of Plant Physiologists

Impaired Photoassimilate Partitioning Caused by Phloem-Specific Removal of Pyrophosphate Can Be Complemented by a Phloem-Specific Cytosolic Yeast-Derived Invertase in Transgenic Plants

Jens Lerchl,[a] Peter Geigenberger,[b] Mark Stitt,[b] and Uwe Sonnewald [a,1]

[a] Institut für Pflanzengenetik und Kulturpflanzenforschung, Corrensstrasse 3, 06466 Gatersleben, Germany
[b] Botanisches Institut der Universität Heidelberg, Im Neuenheimer Feld 360, 69120 Heidelberg, Germany

Constitutive expression of the *Escherichia coli ppa* gene encoding inorganic pyrophosphatase resulted in sugar accumulation in source leaves and stunted growth of transgenic tobacco plants. The reason for this phenotype was hypothesized to be reduced sucrose utilization and loading into the phloem. To study the role of PPi in phloem cells, a chimeric gene was constructed using the phloem-specific *rolC* promoter of *Agrobacterium rhizogenes* to drive the expression of the *ppa* gene. Removal of cytosolic PPi in those cells resulted in photoassimilate accumulation in source leaves, chlorophyll loss, and reduced plant growth. From these data, it was postulated that sucrose hydrolysis via sucrose synthase is essential for assimilate partitioning. To bypass the PPi-dependent sucrose synthase step, transgenic plants were produced that express various levels of the yeast *suc2* gene, which encodes cytosolic invertase, in their phloem cells. To combine the phloem-specific expression of the *ppa* gene and the *suc2* gene, crosses between invertase- and pyrophosphatase-containing transgenic plants were performed. Analysis of their offspring revealed that invertase can complement the phenotypic effects caused by the removal of PPi in phloem cells.

INTRODUCTION

Partitioning and allocation of assimilates play an essential role in plant development and crop yield (Gifford and Evans, 1981). Light-driven carbon dioxide fixation leads to the synthesis of organic carbon. In most higher plants, sucrose is the major transport carbohydrate. It is synthesized in the cytosol of mesophyll cells and translocated via the phloem to sink organs (see Figures 1 and 2).

The comparatively low symplastic connectivity, together with the uphill transport of sucrose due to the concentration gradient between mesophyll and phloem cells, argue for an apoplastic step being involved in phloem loading of most plants (Giaquinta, 1983; Turgeon, 1989). Additional support for this hypothesis comes from an analysis of transgenic plants expressing the *suc2* gene, encoding a yeast-derived invertase targeted to the apoplast (von Schaewen et al., 1990; Dickinson et al., 1991; Heineke et al., 1992). From biochemical data as well as from phenotypic effects, we concluded that apoplastic and therefore carrier-mediated phloem loading occurs in the plants tested (tobacco, tomato, Arabidopsis, and potato). To provide direct evidence for carrier-mediated sucrose transport, Riesmeier et al. (1992, 1993) used a yeast complementation system to isolate a sucrose carrier from spinach and potato. The two proteins from spinach and potato were shown to possess H^+-sucrose symport activities. In situ hybridization experiments demonstrated that the sucrose carrier is expressed in a phloem-specific manner in potato plants (Riesmeier et al., 1993). Interestingly, potato sucrose transporter antisense plants (Riesmeier et al., 1994) revealed a phenotype very similar to that of transgenic plants expressing the *suc2* gene, encoding a yeast-derived apoplastic invertase (Heineke et al., 1992), hinting at the possibility of the manipulation of the same target mechanism.

The proton gradient, which is needed for the proton sucrose cotransport (Delrot and Bonnemain, 1981), is generated by a H^+-ATPase located in the plasma membrane of companion cells (Bouche-Pillon et al., 1994). To maintain an adequate carbon supply, incoming sucrose is cleaved by either invertase or sucrose synthase (Claussen et al., 1985). The role of invertases is still a matter of debate because tissue-specific abundance, compartmentation, and regulation of invertase activities are not well understood. Sucrose synthase, the direct counterpart of the neutral cytosolic invertase (see Figure 2), is known to be directly involved in sucrose cycling in sink tissues (Geigenberger and Stitt, 1993) and in sucrose cleavage and metabolism during glycolysis within the phloem complex of *Ricinus* seedlings (Geigenberger et al., 1993). Phloem specificity of a maize and Arabidopsis sucrose synthase gene was shown in transgenic tobacco plants using the promoter

[1] To whom correspondence should be addressed.

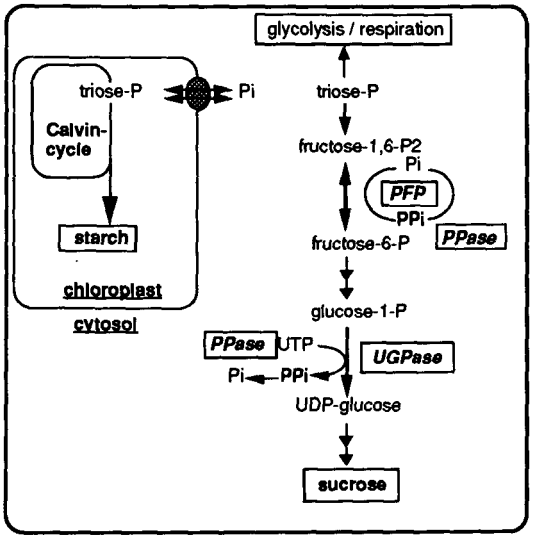

Figure 1. Effects of PPi Removal on Sucrose Biosynthesis in the Cytosol of Photosynthetic Cells.

P, phosphate; P2, bisphosphate; PFP, pyrophosphate:fructose 6-phosphate 1-phosphotransferase; PPase, inorganic pyrophosphatase; UGPase, UDP-glucose pyrophosphorylase.

sequences for the expression of a reporter gene (Yang and Russell, 1990; Martin et al., 1993).

To increase cytosolic sucrose biosynthesis, a PPi-hydrolyzing enzyme from *Escherichia coli* was introduced into the cytosol of transgenic tobacco and potato plants (Jelitto et al., 1992; Sonnewald, 1992). The enzymes PPi:fructose 6-phosphate 1-phosphotransferase (PFP) and the UDP-glucose pyrophosphorylase (UGPase) work near equilibrium. Consequently, a decrease in PPi should prevent the reaction leading to glycolysis and increase sucrose synthesis (see Figure 1). Indeed, plants (named ppa1) expressing the *E. coli ppa* gene, encoding inorganic pyrophosphatase (PPase), driven by the cauliflower mosaic virus (CaMV) 35S promoter showed an increase in UDP-glucose and sucrose content and a decrease in hexose phosphates and PPi content (Jelitto et al., 1992).

Unexpectedly, however, the plants showed stunted growth and reduced root formation, suggesting that in addition to increased sucrose synthesis in leaf mesophyll cells, the export of photoassimilates had been affected. Based on this work, a model was formulated postulating that PPi was essential for sucrose transport (Sonnewald, 1992).

In this study, we investigated the putative role of PPi in phloem metabolism. To this end, the *ppa* gene from *E. coli* was expressed using the phloem-specific *rolC* promoter from *Agrobacterium rhizogenes*. Analysis of the transgenic plants showed that cytosolic PPi is essential for long-distance sucrose transport. To exclude pleiotropic effects, a complementation approach was used. Low levels of a phloem-specific cytosolic invertase activity, which is able to bypass the sucrose synthase step, were introduced into the *ppa*-expressing plants, and the wild-type phenotype was restored.

RESULTS

Construction of a Chimeric Gene for the Phloem-Specific Expression of a PPase and Transformation of Tobacco Plants

A chimeric gene consisting of the *rolC* promoter, the *E. coli ppa* gene, and the octopine synthase polyadenylation signal was constructed to confer phloem-specific PPase activity to transgenic plants (see Methods; Figure 3B). After *A. tumefaciens*–mediated gene transfer, regenerated tobacco plants (subsequently named ppa4) were screened for PPase activity, and 20 preselected plants were transferred into the greenhouse. Three independent transformants were analyzed in more detail.

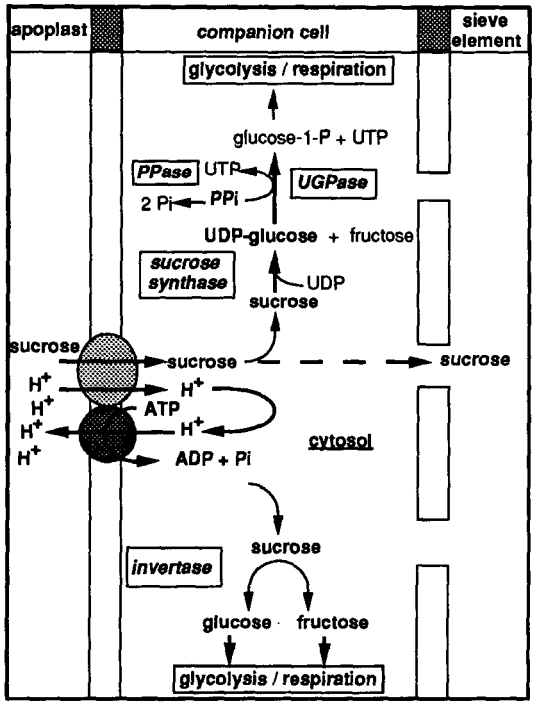

Figure 2. Proposed Model for Pyrophosphate-Dependent, Active Phloem Loading and UDP-glucose Metabolism.

P, phosphate; PFP, pyrophosphate:fructose 6-phosphate 1-phosphotransferase; PPase, inorganic pyrophosphatase; UGPase, UDP-glucose pyrophosphorylase.

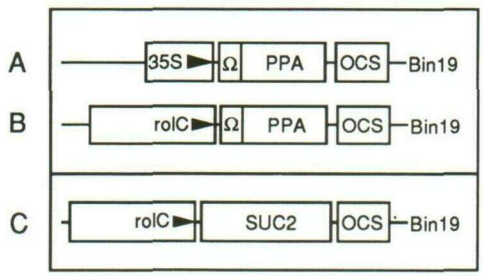

Figure 3. Structure of the Chimeric Binary Plant Expression Cassettes Used for Plant Transformation.

(A) Constitutive expression of the *ppa* gene driven by the CaMV 35S promoter. Ω, 5′ untranslated leader sequence from tobacco mosaic virus strain U1; OCS, octopine synthase poly(A) site.
(B) Phloem-specific expression of the *ppa* gene driven by the *rolC* promoter from *A. rhizogenes*.
(C) Phoem-specific expression of the yeast *suc2* gene driven by the *rolC* promoter.

Immunocytochemical Localization of the PPase Polypeptide in Phloem Cells

To obtain polyclonal antibodies against the PPase polypeptide, the protein was overproduced in *E. coli* (see Methods). The purified protein was used for immunization of rabbits. Polyclonal antibodies were specific for the PPase protein, as determined in immunoblot experiments (data not shown). Polyclonal antibodies were used for the immunocytochemical localization of the PPase protein in leaf cross-sections (see Figures 4A to 4C).

For immunohistochemical detection of the foreign gene product, leaf material of untransformed control, ppa1, and ppa4 plants was embedded in Paraplast Plus media. The PPase protein was subsequently visualized in thin sections following the protocol given in Methods.

As shown in Figure 4A, no indication of antigenic reactions was observed in leaf cross-sections of untransformed control plants, whereas cuttings of ppa1 plants (Figure 4B) showed overall staining (bluish color) of leaf material, indicating constitutive 35S-driven expression of the *ppa* gene (Fang et al., 1989). Even though general staining was observed, a densely stained area was found in the circle of phloem cells. In contrast, the immunolocalization of the PPase protein in leaf cross-sections of ppa4 plants (Figure 4C) revealed a densely stained area in cells of the inner and outer phloem of the midrib and in minor veins, confirming the specificity of the *rolC*-driven expression in phloem cells.

Removal of Cytosolic PPi in Phloem Cells Leads to the Accumulation of Starch in Source Leaves of Transgenic Tobacco Plants

To study the impact of phloem-specific PPase expression on the level of carbohydrates in leaves, the glucose, fructose, sucrose, and starch content of three independent primary ppa4 transformants grown under greenhouse conditions (see Methods) was determined (Table 1). Samples were taken from old mature leaves after 8 hr of illumination. As shown in Table 1, mature leaves of each individual ppa4 transformant accumulated soluble sugars as well as starch when compared with untransformed wild-type plants.

Plants obtained from seed of the individual transformant ppa4 plant 80 were chosen for more detailed analysis and compared with wild-type and ppa1 plants. The accumulation of carbohydrates was determined in four 68-day-old plants after

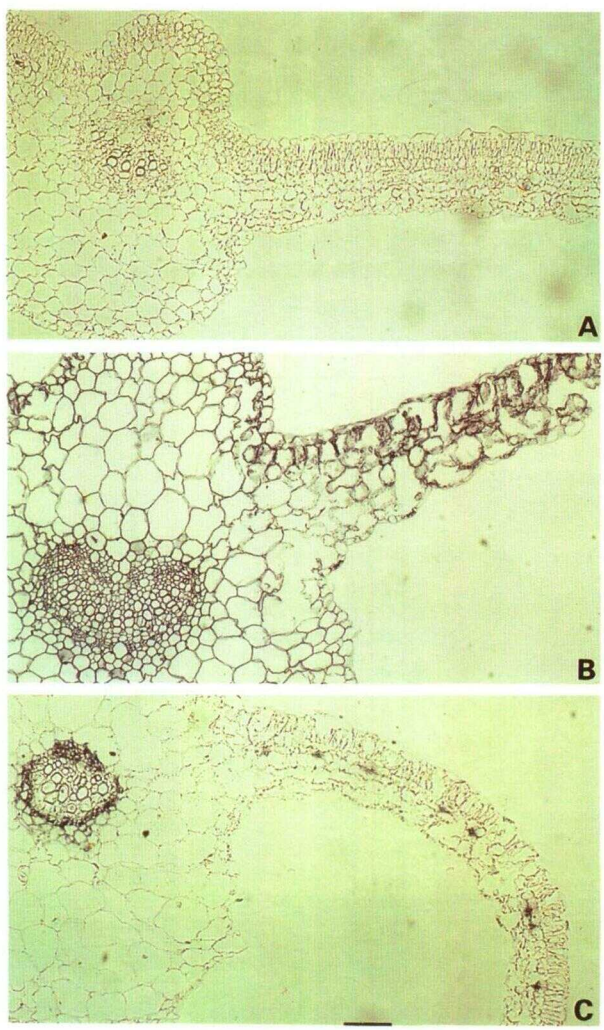

Figure 4. Immunocytochemical Localization of the PPase Protein in Leaf Cross-Sections of Transgenic Plants.

(A) Cross-section of a leaf of an untransformed wild-type plant.
(B) Cross-section of a leaf of a transgenic plant expressing the *E. coli ppa* gene driven by the CaMV 35S promoter.
(C) Cross-section of a leaf of a transgenic plant expressing the *E. coli ppa* gene driven by the *rolC* promoter. Bar = 200 μm.

Table 1. Sugar Accumulation in Leaf Laminae of Transgenic Tobacco Plants Expressing the *E. coli ppa* Gene

	Wild Type	ppa4-80	ppa4-36	ppa4-7
Glucose	66 ± 1	772 ± 10	700 ± 42	1071 ± 94
Fructose	43 ± 1	478 ± 37	449 ± 43	554 ± 39
Sucrose	108 ± 3	221 ± 21	213 ± 21	267 ± 11
Starch	71 ± 3	653 ± 32	570 ± 31	463 ± 31

Values are given as micromoles of hexose per gram fresh weight of tissue ± SE. Values represent results obtained from an old mature leaf. Samples were harvested from 68-day-old plants after 8 hr of illumination. ppa4-7, ppa4-36, and ppa4-80 represent plants 7, 36, and 80, respectively, of the ppa4 transformants.

8 hr of illumination. Because the carbohydrate content varies between developing and mature leaves, samples were taken from the top to the bottom of tobacco plants (see Figure 5). Whereas the soluble sugars glucose, fructose, and sucrose accumulated only in old source leaves of ppa4 plants (Figures 5A to 5C, bars 10 to 12), starch levels were elevated in all leaves, including sink leaves (Figure 5D, bars 1 to 3). This is in contrast to the data obtained from leaves harvested from ppa1 plants, in which soluble sugars accumulated throughout the whole plant, with little or no increase in starch content when compared with wild-type controls (Figure 5).

From the data reported in Figure 5, the sucrose-to-starch ratio found in leaves of ppa1 and ppa4 plants was calculated. As shown in Figure 6, the sucrose-to-starch ratio dramatically increased in leaves of ppa1 plants and decreased in leaves of ppa4 plants.

Removal of PPi Leads to an Accumulation of UDP-Glucose and a Lower ATP-to-ADP Ratio

To ensure the removal of PPi in the cytosol of the transgenic plants, PPi content was determined in leaf laminae and midribs of wild-type, ppa1, and ppa4 plants (Tables 2 and 3). PPi was drastically reduced in both tissues of ppa1 plants, whereas no significant alteration was observed in leaf laminae of ppa4 plants. PPi was slightly decreased in midribs of ppa4 plants; this is remarkable because the effect is restricted to a single cell layer, the phloem cells.

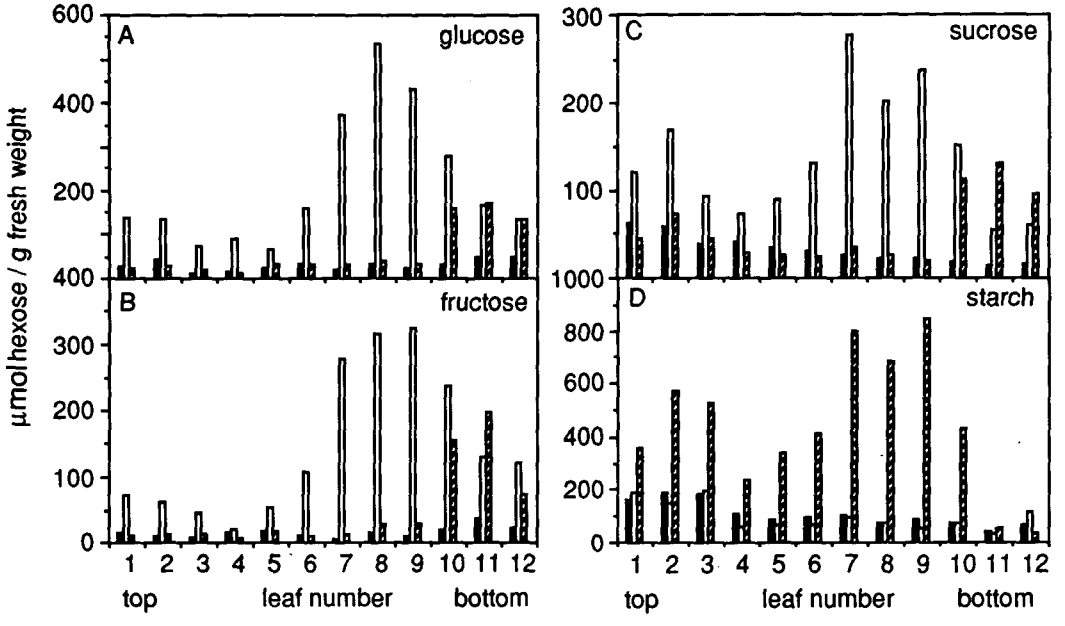

Figure 5. Sugar Content of Leaf Laminae of Transgenic Plants Expressing the *E. coli ppa* Gene.

Values are given as micromoles of hexose per gram fresh weight of tissue. Standard error was less than 5% in each case. Leaf laminae were harvested after 8 hr of illumination from 68-day-old plants grown from seed under greenhouse conditions. Offspring of the individual ppa4 plant 80 were used in the experiment. Black bars represent wild-type values. Open bars represent ppa1 plant values. Hatched bars represent ppa4 plant values.

(A) Glucose content in leaf laminae determined from samples taken continuously from the top to the bottom of the plant (leaves 1 to 12).

(B) Fructose content in leaf laminae.

(C) Sucrose content in leaf laminae.

(D) Starch content in leaf laminae.

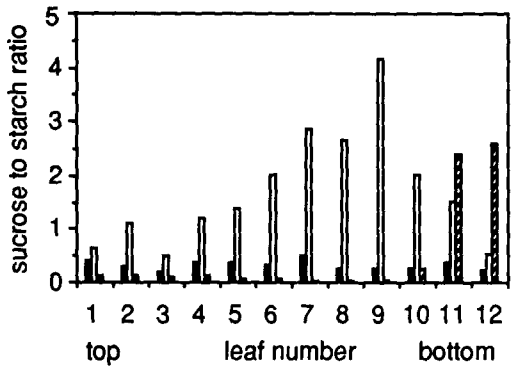

Figure 6. Sucrose-to-Starch Ratios from Leaves of Transgenic Tobacco Plants Expressing the *E. coli ppa* Gene.

Separate sucrose and starch values are given in Figure 5. Black bars represent wild-type values. Open bars represent ppa1 plant values. Hatched bars represent ppa4 plant values.

To provide additional support for the model shown in Figure 2, the UDP-glucose and glucose 1-phosphate levels were determined in leaf laminae and midribs. These sugars can be interconverted via the enzyme UGPase (Figure 1), which is proposed to catalyze a readily reversible reaction in the presence of PPi and UTP. Removal of PPi should therefore lead to the accumulation of UDP-glucose. As shown in Table 2, the UDP-glucose content found in leaf laminae was increased fourfold in ppa1 plants when compared with wild-type plants, whereas no change in UDP-glucose content was found in ppa4 plants. The levels of glucose 1-phosphate were slightly elevated in both transgenic lines (Table 2). In midrib extracts, UDP-glucose content was increased 10-fold in ppa1 plants and fourfold in ppa4 plants as compared with wild-type plants, whereas glucose 1-phosphate content was not altered (Table 3).

To investigate the consequences of phloem-specific PPi removal on the energy status, the levels of ATP, ADP, and AMP in leaf midribs were determined. Although midribs are not the major site of phloem loading, they play an important role during long-distance sucrose transport and the reloading of sucrose along the transport pathway. Sucrose synthase activity was taken as a marker enzyme for phloem-enriched tissue (data not shown). It was determined that the ATP-to-ADP ratio decreased and the AMP levels increased (Table 4). These results support the proposed model because the removal of PPi in phloem cells should lead to reduced ATP production (see Figure 2).

Although metabolite measurements indicate a reduced energy status within the phloem cells, additional secondary effects cannot be ruled out. However, the formation of callose at sieve plates due to elevated UDP-glucose levels in transgenic plants appears unlikely. As estimated by aniline blue staining (Eschrich, 1975) and light microscopy, no increased callose formation was observed from midrib longitudinal sections of transgenic PPase plants compared with wild-type plants (data not shown).

Removal of Cytosolic PPi in Phloem Cells Impairs Normal Plant Development

To analyze the phenotypic changes of tobacco plants expressing the *ppa* gene driven by the phloem-specific *rolC* promoter, transgenic plants were grown in the greenhouse and their growth behavior was studied. ppa4 and ppa1 plants showed stunted growth compared with wild-type plants (Figure 7); however, the leaf number was not altered. Consequently the internode distance expressed as the ratio of plant height-to-leaf number was strongly decreased (see Table 5). Leaves of ppa4 plants underwent increasing chlorophyll loss from the sink-to-source transition, as has been previously observed for ppa1 plants (Figures 7B and 7C; Sonnewald, 1992). The length and width of the leaves were determined (Figure 8). Whereas older leaves (leaves numbered 5 to 9 in Figures 8A and 8B) were shorter than the corresponding wild-type leaves, young and developing leaves were not significantly altered (Figures 8A and 8B, leaves numbered 1 to 4). The oldest leaves numbered 10 to 12 were less affected than leaves numbered 5 to 9 (Figures 8A and 8B). In general, phenotypic changes in ppa1 plants were more pronounced than were those in ppa4 plants.

Phloem-Specific Localization of Yeast Invertase in Transgenic Tobacco Plants Has No Detrimental Effect on Plant Growth

A plant expression cassette containing the *rolC* promoter and the octopine synthase polyadenylation signal based on the vector pBin19 (Bevan, 1984) was used to introduce the *suc2* gene from yeast (Taussig and Carlson, 1983) via *A. tumefaciens*–mediated gene transfer (see Figure 3C). The regenerated plants (subsequently named IN8) contained cytosolic yeast-derived invertase activity in phloem cells. Fifty transgenic tobacco plants bearing the *rolC-suc2* construct were screened for

Table 2. Contents of Marker Molecules of Sucrose Biosynthesis from Transgenic Tobacco Plants Expressing the *E. coli ppa* Gene Determined from Leaf Laminae

Metabolite	Wild Type	ppa1	ppa4
UDP-glucose	36.1 ± 4.3	134 ± 8	31 ± 3.7
Glucose 1-phosphate	13.7 ± 1.8	19.6 ± 2.9	19.2 ± 4.1
PPi	11.0 ± 2.1	2.2 ± 0.3	10.8 ± 3.2
Glucose 1-phosphate/ UDP-glucose	0.38 ± 0.02	0.14 ± 0.01	0.62 ± 0.12

Values are given as nanomoles per gram fresh weight of tissue. Leaf laminae were harvested after 8 hr of illumination from 87-day-old plants grown from seed of the F_2 generation. Offspring of ppa4 plant 80 were used in the experiment. Values are the mean ± SE of four plants.

Table 3. Contents of Marker Molecules of Sucrose Biosynthesis from Transgenic Tobacco Plants Expressing the *E. coli ppa* Gene Determined from Midribs

Metabolite	Wild Type	ppa1	ppa4
UDP-glucose	12.9 ± 2.0	124 ± 4	43.5 ± 7.9
Glucose 1-phosphate	6.1 ± 0.6	6.9 ± 0.8	6.6 ± 0.7
PPi	2.4 ± 0.2	<0.2	1.5 ± 0.4
Glucose 1-phosphate/ UDP-glucose	0.47 ± 0.14	0.06 ± 0.01	0.15 ± 0.02

Values are given as nanomoles per gram fresh weight of tissue. Midribs were harvested after 8 hr of illumination from 87-day-old plants grown from seeds of the F_2 generation. Offspring of ppa4 plant 80 were used in the experiment. Values are the mean ± SE of four plants.

enzymatic activity in midribs using an invertase activity gel (von Schaewen et al., 1990; data not shown). Twenty-four preselected plants were transferred to the greenhouse. No detrimental effects on plant growth or development were observed for greenhouse-grown IN8 plants as compared with the wild-type controls (see Figures 9D to 9F). Furthermore, no obvious changes were seen in the steady state content of glucose, fructose, sucrose, or starch (data not shown), even when high invertase activity was present in phloem cells of transgenic plants.

Low Levels of Yeast invertase Activities in the Cytosol of Phloem Cells Can Bypass the Inhibition of PPi-Dependent Sucrose Breakdown via Sucrose Synthase

Phloem-specific reduction of PPi levels strongly influences plant growth, whereas phloem-specific hydrolysis of sucrose in the cytosol has no effect. According to the model, phenotypic changes observed in ppa4 plants are caused by impaired sucrose hydrolysis via sucrose synthase. Thus, introducing an alternative pathway for sucrose hydrolysis in phloem cells should circumvent this metabolic block. To this end, a wild-type plant and three plants containing low (IN8-4), middle (IN8-16), and high (IN8-35) phloem-specific cytosolic yeast-derived invertase activity (Figure 9) were crossed with a ppa4 plant derived from the F_3 generation. The plant population used for the crossing was homozygous with respect to growth behavior, phenotype, and PPase abundance (data not shown).

Twenty offspring from each cross were analyzed for the presence of the PPase protein, invertase activity, and plant growth. As expected, all plants tested showed the same amount of PPase protein in protein gel blot experiments. An example is given in Figure 10. The offspring of the cross between a wild-type and a ppa4 plant (control × ppa4; Figure 9B) grew slightly better than homozygous ppa4 plants (see Figure 9C). The progenies of the selfed invertase plants (IN8) are indistinguishable from wild-type plants (Figures 9D to 9F).

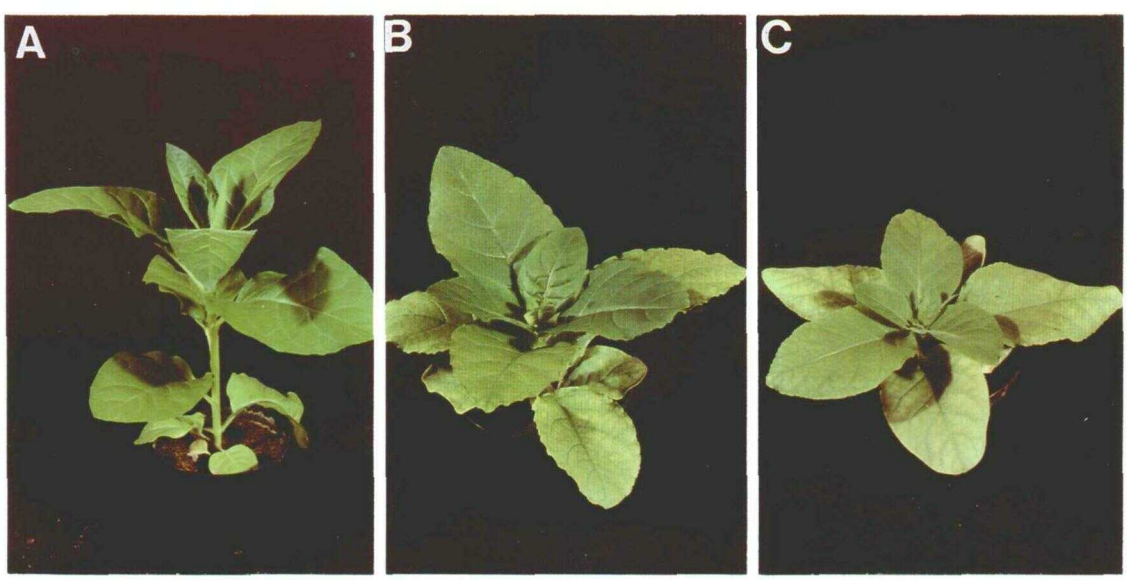

Figure 7. Phenotype of Transgenic Plants Expressing the *E. coli ppa* Gene.

Plants were grown under greenhouse conditions.
(A) A wild-type plant.
(B) A transgenic plant expressing the *ppa* gene driven by the *rolC* promoter.
(C) A transgenic plant expressing the *ppa* gene driven by the CaMV 35S promoter.

Table 4. Content of ATP, ADP, and AMP and the ATP-to-ADP Ratio Determined from Midribs of Transgenic Plants Expressing the *E. coli ppa* Gene

Metabolite	Wild Type	ppa1	ppa4
ATP	22.1 ± 1.4	13.5 ± 4.1	20.9 ± 2.9
ADP	4.7 ± 0.6	15.1 ± 2.9	9.2 ± 1.2
AMP	2.6 ± 0.2	6.9 ± 2.2	3.5 ± 0.3
ATP/ADP	4.7 ± 0.7	0.9 ± 0.1	2.3 ± 0.3

Values are given as nanomoles per gram fresh weight of tissue. Midribs were harvested after 8 hr of illumination from 87-day-old plants grown from seed of the F_2 generation. Offspring of ppa4 plant 80 were used in the experiment. Values are the mean ± SE of four plants.

As shown in Figure 9, depending on the amount of invertase activity (see Figure 11), the wild-type phenotype can be restored in *ppa*-expressing plants. Whereas low invertase activity (ppa4 × IN8 plant 4; Figures 9G and 11) leads to wild-type growth and a reversion of the ppa4 phenotype, plants showing mid-range invertase activity (ppa4 × IN8 plant 16; Figures 9H and 11) were not complemented with respect to ppa4 growth behavior. High invertase activity (ppa4 × IN8 plant 35; see Figures 9I and 11) in combination with the PPase protein reinforced the phenotype up to complete growth inhibition (data not shown). These effects are consistent within the analyzed progeny of each transgenic line.

DISCUSSION

Transgenic Plants Expressing *E. coli ppa* and Yeast *suc2* Genes in a Phloem-Specific Manner

To study the impact of altered PPi and sucrose metabolism on photoassimilate partitioning in phloem cells of transgenic plants, two chimeric genes conferring either phloem-specific PPase (ppa4) or phloem-specific cytosolic invertase (IN8) activity were constructed. Based on the published data obtained with ppa1 plants (Sonnewald, 1992), speculation was that assimilate partitioning would be impaired in ppa4 plants. As expected, ppa4 plants showed stunted growth, chlorophyll loss, and reduced leaf size. The stunted growth was caused by reduced internode distance with no changes in leaf number (Table 5). To confirm the hypothesis outlined in Figure 2, the carbohydrate content in leaves of ppa1 and ppa4 plants was determined. As shown in Figure 5, plants of both transgenic lines accumulate carbohydrates in their leaves. In leaves of ppa4 plants, mainly starch accumulated, whereas in leaves of ppa1 plants, mainly soluble sugars (fructose, glucose, and sucrose) were found to accumulate. The observed difference between the two different *ppa*-expressing plant lines is in agreement with the proposed function of the different cell types involved, namely, the mesophyll and phloem cells. Due to the removal of PPi in mesophyll cells (ppa1 plants), photoassimilate flow is directed toward sucrose synthesis (Figure 1), resulting in a higher sucrose-to-starch ratio in these leaves (Figure 6).

Starch accumulation is found in source leaves if the rate of photosynthesis exceeds the capacity of sink tissues (Stitt, 1991). Due to the removal of PPi in phloem cells, the export of assimilates was inhibited, thus a sink limitation was mimicked, leading to a strong accumulation of starch in leaf mesophyll cells. Finally, the sucrose-to-starch ratio was dramatically decreased (Figure 6). This result can be taken as evidence that the sucrose metabolism in ppa4 plants is not affected in mesophyll cells.

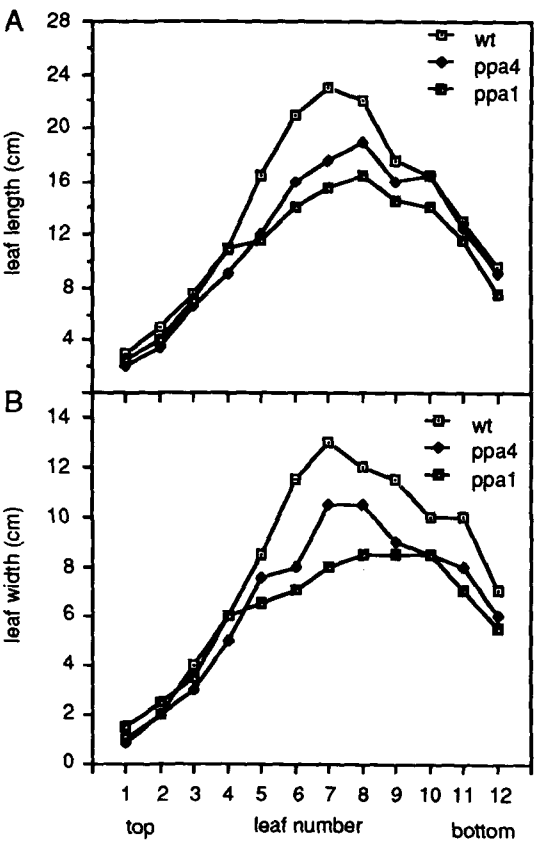

Figure 8. Leaf Length and Width of Transgenic Plants Expressing the *E. coli ppa* Gene.

Plants were grown from seed under greenhouse conditions for 68 days. Leaves were counted from the top to the bottom of the plant (leaves 1 to 12). Standard error was less than 5% using four plants of each genotype in the experiment.

(A) Leaf length of transgenic plants expressing the *ppa* gene.

(B) Leaf width of transgenic plants expressing the *ppa* gene.

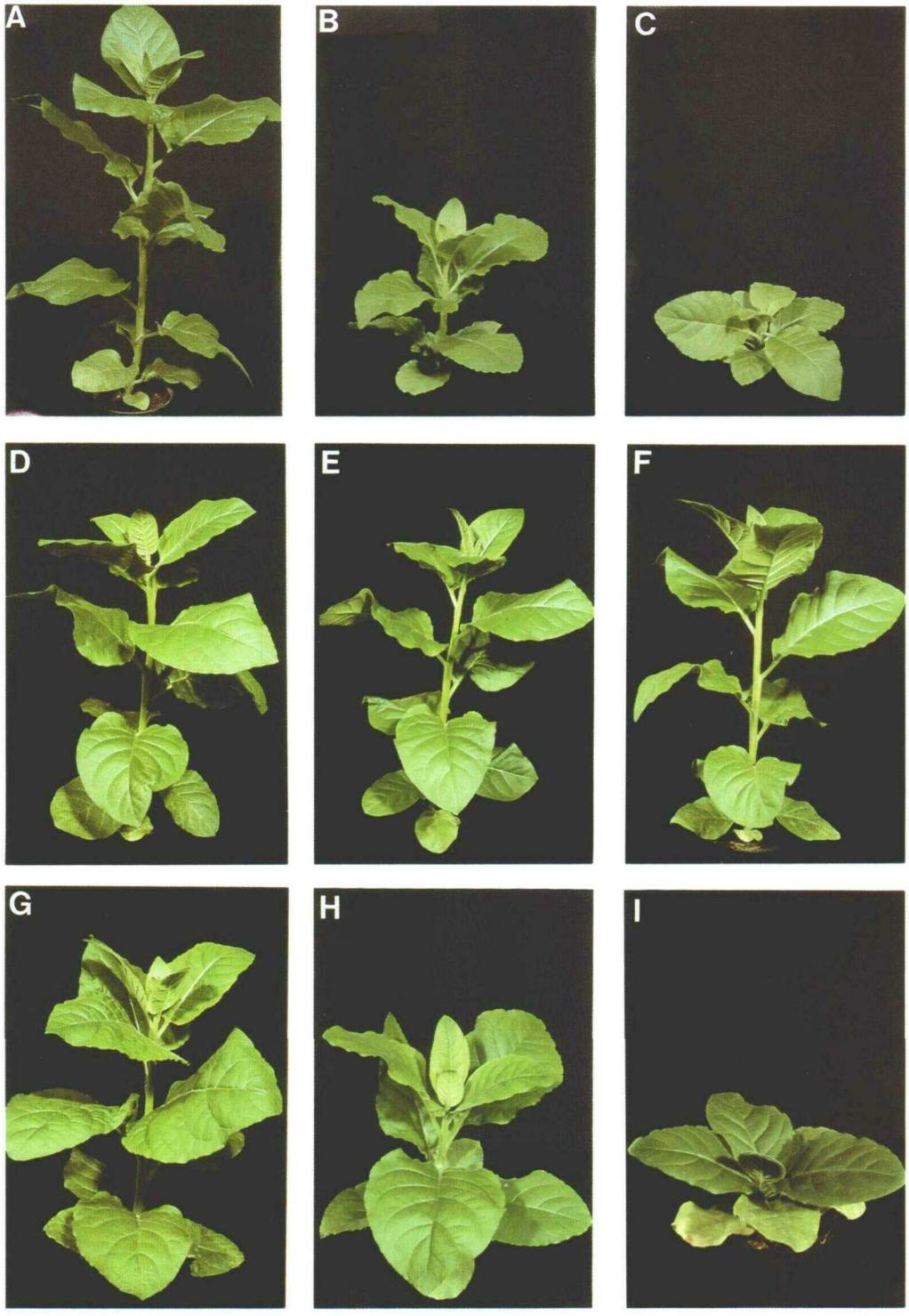

Figure 9. Tobacco Plants of the Progeny Resulting from a Cross between Plants Expressing the *E. coli ppa* Gene and the Yeast *suc2* Gene Driven by the *rolC* Promoter.

(A) A wild-type control.
(B) An offspring of a wild-type plant crossed with a plant expressing the *ppa* gene in the F_3 generation.
(C) A plant obtained from seed of a selfed plant expressing the *ppa* gene in the F_3 generation.
(D) to **(F)** Plants 4, 16, and 35, respectively, of transgenic line IN8 expressing the yeast *suc2* gene encoding cytosolic yeast-derived invertase.
(G) to **(I)** Plants obtained from a cross between a plant expressing the *ppa* gene and plants 4, 16, and 35, respectively, of the primary transformants of transgenic line IN8.

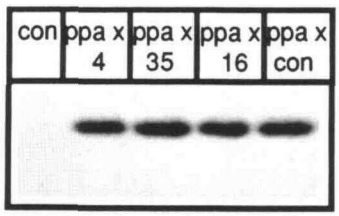

Figure 10. Protein Gel Blot Analysis Showing the Abundance of PPase in Midribs of the Offspring of Transgenic Tobacco Plants after Crossing Transgenic Lines ppa4 and IN8.

Twenty micrograms of soluble protein from midrib extracts of tobacco plants was separated in a 12.5% SDS–polyacrylamide gel followed by electroblotting and immunodetection (see Methods). Con, untransformed wild type; ppa × 4, ppa4 plant 80 × IN8 plant 4; ppa × 35, ppa4 plant 80 × IN8 plant 35; ppa × 16, ppa4 plant 80 × IN8 plant 16; ppa × con, ppa plant 80 × the untransformed wild type.

Expression of the *E. coli ppa* Gene in Phloem Cells of Transgenic Tobacco Plants Leads to Lower PPi Content and Changes in Metabolite Levels

To verify the proposed metabolic changes caused by the activity of the PPase protein, PPi, adenosine nucleotide, UDP-glucose, and glucose 1-phosphate content was determined in leaf laminae and midribs of wild-type, ppa1, and ppa4 plants (Tables 2, 3, and 4).

In ppa1 plants, PPi content was reduced in both tissues investigated, that is, leaf laminae and midribs. This reduction was accompanied by a severalfold decrease in the ratio of glucose 1-phosphate to UDP-glucose when compared with wild-type plants. In ppa4 plants, PPi content was specifically reduced in midribs. Whereas the ratio of glucose 1-phosphate to UDP-glucose increased slightly in leaf laminae of ppa4 plants, the mean value was reduced threefold in midribs.

In contrast to photosynthetically active mesophyll cells, in phloem tissues sucrose cleavage is dominant over resynthesis. Consequently, the preferred action of UGPase activity should work in different directions in these two tissues. The consequences are illustrated in Figure 2, which represents a PPi-dependent mechanism of sucrose utilization. Sucrose must be transported actively against a concentration gradient via the apoplast into companion cells. The transport process is believed to be a proton–sucrose symport. The established proton gradient can be maintained only by ATP cleavage. To guarantee adequate ATP recycling, incoming sucrose must be cleaved by the activity of either sucrose synthase or invertases, and the products must be metabolized during glycolysis and the citric acid cycle. The products of sucrose synthase activity are fructose and UDP-glucose. Fructose can be metabolized by fructokinases, whereas UDP-glucose must be converted to glucose 1-phosphate by the action of UGPase. This PPi-dependent step is inhibited due to the activity of PPase in transgenic plants. Thus, UDP-glucose cannot be catabolized, leading to an impaired energy status that consequently inhibits active transport processes.

Interestingly, enzymatic activities involved in glycolysis and sucrose biosynthesis (pyruvate kinase, plastidic fructose 1,6-bisphosphatase, plastidic and cytoplasmic aldolase, UGPase, and PPi:fructose 6-phosphate 1-phosphotransferase) do not show significant changes (data not shown).

Phenotypic Changes Caused by the Phloem-Specific Expression of the *E. coli ppa* Gene Can Be Complemented by the Phloem-Specific Expression of the *suc2* Gene from Yeast in Transgenic Tobacco Plants

Phloem-specific expression of the *E. coli ppa* gene resulted in starch accumulation in source leaves and stunted growth of transgenic tobacco plants. The reason for this phenotype was hypothesized to be reduced sucrose loading into the phloem (Figure 2). It was further postulated that to maintain a proton gradient across the plasma membrane of companion cells, a small proportion of the incoming sucrose had to be hydrolyzed via sucrose synthase in the phloem tissue. A decrease of cytosolic PPi would reduce the energy gain and thereby inhibit long-distance sucrose transport, resulting in sugar accumulation in source leaves. To circumvent the sucrose synthase pathway, a new sucrose hydrolytic activity, yeast invertase, was introduced into the phloem cells of transgenic tobacco plants. Invertase-expressing tobacco plants were crossed with ppa4 plants, and the growth behavior of the offspring was analyzed in the greenhouse. Depending on the amount of invertase activity, the wild-type phenotype could be restored in transgenic plants expressing the *ppa* gene.

From these data, we concluded that cytosolic invertase can bypass the sucrose synthase pathway in phloem cells. A high level of PPase activity in phloem cells did not severely affect plant development if an alternative sucrose hydrolytic activity was present. Therefore, unspecific dephosphorylation or

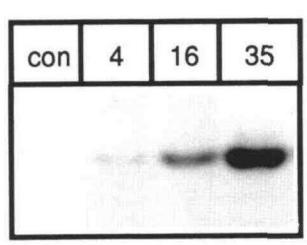

Figure 11. An Invertase Activity Gel Showing Invertase Activity in Individual Plants 4, 16, and 35 of Transgenic Line IN8 Expressing the *rolC*-Driven Yeast *suc2* Gene Encoding Cytosolic Invertase.

Twenty micrograms of soluble protein from midrib extracts of tobacco plants was separated in a 12.5% SDS–polyacrylamide gel without prior boiling of protein extracts (see Methods). Con, untransformed wild type; 4, transgenic line IN8 plant 4; 16, IN8 plant 16; 35, IN8 plant 35.

Table 5. Internode Distance as the Ratio of Plant Height to Leaf Number in Transgenic Plants Expressing the *E. coli ppa* Gene

	Wild Type	ppa4	ppa1
Height (cm)	24	11	3.5
Leaf number	12	12	12
Internode length	2	0.92	0.29

Plants were grown from seed under greenhouse conditions (see Methods). Standard error was less than 5% using four 68-day-old plants in the experiment.

pleiotropic effects due to *ppa* gene expression can be excluded. Furthermore, our results demonstrated that sucrose hydrolysis must be tightly controlled because high cytosolic invertase activities led to severe growth injuries in combination with PPase abundance.

Conclusion

Our data show that removal of PPi in phloem cells results in photoassimilate accumulation in leaves and reduced growth of the plants. *ppa* gene expression is specific and can be bypassed by low levels of invertase activity. Phenotypic alterations and physiological data indicate that long-distance transport processes are PPi dependent. The measured decrease in the ATP-to-ADP ratio in midribs indicates that glycolysis and respiration are impaired in this tissue, suggesting that the H^+-gradient across the plasmalemma cannot be maintained or established in a manner adequate to allow sucrose transport. A reduced respiration rate in midribs of plants expressing the *ppa* gene was measured by Geigenberger et al. (1995); this supports the idea of an impaired energy status in phloem tissue and transport processes. Current work is now focused on a more detailed physiological analysis of transgenic plants with respect to plant development as well as nitrogen metabolism and long-distance sucrose transport.

METHODS

Plants, Bacterial Strains, and Media

Tobacco (*Nicotiana tabacum* cv Samsun NN) plants were obtained through Vereinigte Saatzuchten eG, Ebstorf, Germany. Plants in tissue culture were grown under a 16-hr-light/8-hr-dark regime on Murashige and Skoog medium (Murashige and Skoog, 1962) containing 2% sucrose. Plants for biochemical analysis were grown in the greenhouse under a 16-hr-light/8-hr-dark regime for 87 days after germination. *Escherichia coli* strain XL-1 Blue (Bullock et al., 1987) was cultivated using standard techniques (Sambrook et al., 1989). *Agrobacterium tumefaciens* C58C1 containing pGV2260 (Deblaere et al., 1984) was cultivated in YEB medium (Vervliet et al., 1975).

Reagents

DNA restriction and modification enzymes were obtained from Boehringer Mannheim and GIBCO. Synthetic oligonucleotides were synthesized on a DNA synthesizer (model 380A; Applied Biosystems, Foster City, CA). Reagents for SDS-PAGE were purchased from Bio-Rad. Chemicals were obtained through Sigma or Merck.

Construction of Chimeric Plasmids

The *rolC* promoter from *A. rhizogenes* was cloned by polymerase chain reaction (PCR) following the instructions of the manufacturer (Perkin-Elmer, Ueberlingen, Germany). The temperature profile of the PCR cycle (40 cycles) was as follows: 1 min at 95°C, 1 min at 45°C, and 2 min at 72°C. Plasmid DNA containing the *rolC* promoter was isolated from *A. rhizogenes* bearing the plasmid pABC002 (Schmülling et al., 1989) using standard procedures (Sambrook et al., 1989). Synthetic oligonucleotides were synthesized based on the published sequence of the *rolC* promoter fragment (Slightom et al., 1986). The sequences of the primers are as follows: the 5′ *rolC* primer, d(GGAATTCGATACGAAAAAGGCAAGTGCCAGGGCC); and the 3′ *rolC* primer, d(CCCATGGTACCCCATAACTCGAAGCATCC). The amplified DNA was cloned into the PCR vector pCR1000 (Invitrogen, Norwalk, CT). To exclude mutations of the amplified DNA during the PCR cycles, the clone was sequenced using the dideoxy method (Sanger et al., 1977). The 1150-bp promoter fragment was subsequently cloned into a plant expression cassette (Sonnewald, 1992) by replacement of the cauliflower mosaic virus (CaMV) 35S promoter sequence (Franck et al., 1980) through the *rolC* promoter (Figure 3) by using the 5′ restriction site of EcoRI and the 3′ restriction site of Asp718 included in the PCR primers. The final construct was based on the binary vector pBin19 (Bevan, 1984). The resulting plasmid contained the *ppa* gene (Lathi et al., 1988) and a translation enhancer (Gallie et al., 1987) between the *rolC* promoter and the octopine synthase polyadenylation signal (Gielen et al., 1984).

Metabolite Determination

All metabolites were measured photometrically using the ZFP spectrophotometer (Sigma). UDP-glucose content and glucose 1-phosphate content were determined as described by Stitt et al. (1984); nucleotides were determined following a protocol described by Stitt et al. (1982). PPi was measured according to Weiner et al. (1987).

Plant Transformation

Plant transformation using the *Agrobacterium*-mediated gene transfer for tobacco was as described by Rosahl et al. (1987).

RNA Gel Blot Analysis

Total RNA isolation and gel electrophoresis were done according to Logemann et al. (1987). RNA gel blot hybridization was performed as described by Amasino (1986).

Overexpression and Purification of Inorganic Pyrophosphatase

The *ppa* gene was subcloned into the blunt-ended BamHI restriction site of the overexpression vector pQE9 (Diagen, Hilden, Germany) as a blunt-ended NcoI-SalI fragment (Sonnewald, 1992) using T4 DNA polymerase (Boehringer Mannheim). The overexpression and purification of the gene product were performed following a standard protocol of the manufacturer, using an N-terminal histidine tag for one-step purification of the protein. Antibodies were raised against the inorganic pyrophosphatase (PPase) by immunizing rabbits.

Protein Gel Blot Analysis

After separation in a 15% SDS–polyacrylamide gel (Laemmli, 1970), proteins were transferred onto nitrocellulose membranes (Millipore, Bedford, MA) using a semidry electroblotting apparatus (Multiphore II; LKB, Bromma, Sweden). After blocking with 3% BSA in TBS (50 mM Tris-HCl, pH 7.4, 500 mM sodium chloride), the membrane was incubated for 1 hr at room temperature with the anti-PPase antibody at a 1:1000 dilution containing 1% BSA in TBS. For the following immunochemical detection procedure, the biotin–streptavidin system from Amersham Buchler (Braunschweig, Germany) was used with anti-rabbit biotinylated species-specific whole antibody from donkey and streptavidin-biotinylated horseradish peroxidase.

Preparation of Cuttings for Immunohistochemical Staining

Fixation and dehydration were done according to Angerer and Angerer (1992) using 1-cm midrib cuttings carried over for 1 hr in a fixative containing 2.5% glutaraldehyde and 50 mM sodium cacodylate trihydrate, pH 7.0. Tissue was vacuum infiltrated two times using fresh fixative. Paraplast Plus (Sherwood Medical, St. Louis, MO) was used for embedding. Cuttings (15-μm) were prepared using a microtome (model HM400; Microm, Heidelberg, Germany) and placed on polylysine-coated microscope slides (Sigma) until use. Paraplast was removed from slides by incubation for 5 min in 100% xylene following a 25% stepwise decrease of xylene in ethanol and 25% stepwise increase of ethanol, ending in TBS containing 50 mM Tris-HCl, pH 7.4, and 500 mM sodium chloride. Cuttings were blocked at room temperature for 30 min using 3% BSA in TBS containing 0.1% Tween 20. The anti-PPase antibody was used at a 1:1000 dilution, and cuttings were incubated for 1 hr at 37°C. The cuttings were washed three times for 2 min in TBS. For the following immunocytochemical detection procedure, the biotin–streptavidin system from Amersham Buchler was used with anti-rabbit biotinylated species-specific whole antibody from donkey (1:1000 dilution in TBS, incubation for 1 hr at 37°C) and streptavidin-biotinylated alkaline phosphatase (1:1000 dilution in TBS, incubation for 30 min at 37°C).

Determination of Soluble Sugars and Starch

Leaf discs were extracted with 80% ethanol (10 mM *N*-[2-hydroxyethyl]piperazine-*N'*-[2-ethanesulfonic acid], pH 7.4) at 80°C for 1 to 2 hr. The supernatant was used to determine glucose, fructose, and sucrose content (Stitt et al., 1989). The pellet of the leaf lamina was extracted a second time, washed in water, and dried. Determination of starch content was accomplished using a starch determination kit (Boehringer Mannheim).

Invertase Activity Gel Analysis

Activity staining of yeast-derived invertase was performed as described by von Schaewen et al. (1990). Nonboiled midrib protein extracts were separated on a 10% SDS–polyacrylamide gel using standard protein sample buffer (Sambrook et al., 1989) without SDS.

ACKNOWLEDGMENTS

We thank Andrea Knospe for taking care of tissue culture; Ludmilla Borisjuk and Renate Manteuffel for help during antibody production and histochemical preparations; Heike Ernst and Birgit Schäfer for photographic work; and Hellmuth Fromme, Christoph Bürger, and the greenhouse personnel for care of plants. We also thank Karin Herbers for her help during the preparation of the manuscript. This work was supported by the Deutsche Forschungsgemeinschaft (DFG; Grant No. So 300/1-1) and the Bundesministerium für Forschung und Technologie (BMFT; Grant No. 0310060A).

Received October 24, 1994; accepted January 20, 1995.

REFERENCES

Amasino, R.M. (1986). Acceleration of nucleic acid hybridization rate by polyethylene glycol. Anal. Biochem. **152,** 304–307.

Angerer, L.M., and Angerer, R.C. (1992). In situ hybridization to cellular RNA probes. In In Situ Hybridization, a Practical Approach, D.G. Wilkinson, ed (Oxford, UK: Oxford University Press/IRL Press), pp. 14–32.

Bevan, M. (1984). Binary *Agrobacterium* vectors for plant transformation. Nucl. Acids Res. **12,** 8711–8721.

Bouche-Pillon, S., Fleurat-Lessard, P., Fromont, J.C., Serrano, R., and Bonnemain, J.L. (1994). Immunolocalization of the plasma membrane H^+-ATPase in minor veins of *Vicia faba* in relation to phloem loading. Plant Physiol. **105,** 691–697.

Bullock, W.O., Fernandez, J.M., and Short, J.M. (1987). XL-1 Blue: A high efficiency plasmid transforming *recA Escherichia coli* strain with β-galactosidase selection. BioTechniques **5,** 376–378.

Claussen, W., Loveys, B.R., and Hawker, J.S. (1985). Comparative investigations on the distribution of sucrose synthase activity and invertase activity within growing, mature and old leaves of some C3 and C4 plant species. Physiol. Plant. **65,** 275–280.

Deblaere, R., Bytebier, B., de Greve, H., Debroeck, F., Schell, J., Van Montagu, M., and Leemans, J. (1984). Efficient octopine Ti plasmid-derived vectors of *Agrobacterium*-mediated gene transfer to plants. Nucl. Acids Res. **13,** 4777–4788.

Delrot, S., and Bonnemain, L.L. (1981). Involvement of protons as a substrate for the sucrose carrier during phloem loading in *Vicia faba* leaves. Plant Physiol. **67,** 560–564.

Dickinson, C.D., Altabella, T., and Chrispeels, M.J. (1991). Slow-growth phenotype of transgenic tomato plants expressing apoplastic invertase. Plant Physiol. **95,** 420–425.

Eschrich, W. (1975). Sealing systems in phloem. In Encyclopedia of Plant Physiology, Vol. 1., M.H. Zimmermann and J.A. Milburn, eds (Berlin: Springer Verlag), pp. 39–56.

Fang, R.-X., Nagy, F., Sivasubramaniam, S., and Chua, N.-H. (1989). Multiple *cis* regulatory elements for maximal expression of the cauliflower mosaic virus 35S promoter in transgenic plants. Plant Cell **1**, 141–150.

Franck, A., Guilley, H., Jonard, G., Richards, K., and Hirth, L. (1980). Nucleotide sequence of cauliflower mosaic virus DNA. Cell **21**, 285–294.

Gallie, D.R., Watts, J.W., Turner, P.C., and Wilson, A. (1987). A comparison of eucaryotic viral 5′-leader sequences as enhancers of mRNA expression *in vivo*. Nucl. Acids Res. **15**, 8693–8711.

Geigenberger, P., and Stitt, M. (1993). Sucrose synthase catalyses a readily reversible reaction in vivo in developing potato tubers and other plant tissues. Planta **189**, 329–339.

Geigenberger, P., Langenberger, S., Wilke, I., Heineke, D., Heldt, H.W., and Stitt, M. (1993). Sucrose is metabolised by sucrose synthase and glycolysis within the phloem of *Ricinus communis* L. seedlings. Planta **190**, 446–452.

Geigenberger, P., Lerchl, J., Stitt, M., and Sonnewald, U. (1995). Phloem-specific expression of pyrophosphatase inhibits long distance transport of carbohydrates and amino acids in tobacco plants. Plant Cell Environ., in press.

Giaquinta, R.T. (1983). Phloem loading of sucrose. Annu. Rev. Plant Physiol. **34**, 347–387.

Gielen, J., de Beuckeleer, M., Seurinck, J., Debroeck, H., de Greve, H., Lemmers, M., Van Montagu, M., and Schell, J. (1984). The complete nucleotide sequence of the TL-DNA of the *Agrobacterium tumefaciens* plasmid pTiAch5. EMBO J. **3**, 835–846.

Gifford, R.M., and Evans, L.T. (1981). Photosynthesis, carbon partitioning and yield. Annu. Rev. Plant Physiol. **32**, 485–509.

Heineke, D., Sonnewald, U., Büssis, D., Günter, G., Leidreiter, K., Wilke, I., Raschke, K., Willmitzer, L., and Heldt, H.W. (1992). Apoplastic expression of yeast-derived invertase in potato: Effects on photosynthesis, leaf solute composition, water relation, and tuber composition. Plant Physiol. **100**, 301–308.

Jelitto, T., Sonnewald, U., Willmitzer, L., Hajirezaei, M., and Stitt, M. (1992). Inorganic pyrophosphate content and metabolites in leaves and tubers of potato and tobacco plants expressing *E. coli* pyrophosphatase in their cytosol: Biochemical evidence that sucrose metabolism has been manipulated. Planta **188**, 238–244.

Laemmli, U.K. (1970). Cleavage of structural proteins during assembly of the head of bacteriophage T4. Nature **227**, 680–685.

Lathi, R., Pitkaranta, T., Valve, E., Ilta, I., Kukko-Kalske, E., and Heinonen, J. (1988). Cloning and characterization of the gene encoding inorganic pyrophosphatase of *Escherichia coli* K-12. J. Bacteriol. **170**, 5901–5907.

Logemann, J., Schell, J., and Willmitzer, L. (1987). Improved method for the isolation of RNA from plant tissues. Anal. Biochem. **163**, 21–26.

Martin, T., Frommer, W.B., Salanoubat, M., and Willmitzer, L. (1993). Expression of an *Arabidopsis* sucrose synthase gene indicates a role in metabolization of sucrose both during phloem loading and in sink organs. Plant J. **4**, 367–377.

Murashige, T., and Skoog, F. (1962). A revised medium for rapid growth and bioassays with tobacco tissue cultures. Physiol. Plant. **15**, 473–497.

Riesmeier, J.W., Willmitzer, L., and Frommer, W.B. (1992). Isolation and characterization of a sucrose carrier cDNA from spinach by functional expression in yeast. EMBO J. **11**, 4705–4713.

Riesmeier, J.W., Hirner, B., and Frommer, W.B. (1993). Potato sucrose transporter expression in minor veins indicates a role in phloem loading. Plant Cell **5**, 1591–1598.

Riesmeier, J.W., Frommer, W.B., and Willmitzer, L. (1994). Evidence for an essential role of the sucrose transporter in phloem loading and assimilate partitioning. EMBO J. **13**, 1–7.

Rosahl, S., Schell, J., and Willmitzer, L. (1987). Expression of a tuber-specific storage protein in transgenic tobacco plants: Demonstration of an esterase activity. EMBO J. **6**, 23–29.

Sambrook, J., Maniatis, T., and Fritsch, E.F. (1989). Molecular Cloning: A Laboratory Manual. (Cold Spring Harbor, NY: Cold Spring Harbor Laboratory Press).

Sanger, F., Nicklen, S., and Coulson, A.R. (1977). DNA sequencing with chain-terminating inhibitors. Proc. Natl. Acad. Sci. USA **74**, 5463–5467.

Schmülling, T., Schell, J., and Spena, A. (1989). Promoters of the *rolA*, *B*, and *C* genes of *Agrobacterium rhizogenes* are differentially regulated in transgenic plants. Plant Cell **1**, 665–670.

Slightom, J.L., Durand-Tardif, M., Jouanin, L., and Tepfer, D. (1986). Nucleotide sequence of TL-DNA of *Agrobacterium rhizogenes* agropine type plasmid. J. Biol. Chem. **261**, 108–121.

Sonnewald, U. (1992). Expression of *E. coli* inorganic pyrophosphatase in transgenic plants alters photoassimilate partitioning. Plant J. **2**, 571–581.

Stitt, M. (1991). Rising CO_2 levels and their potential significance for carbon flow in photosynthetic cells. Plant Cell Environ. **14**, 741–762.

Stitt, M., Mieskes, G., Soling, H.D., and Heldt, H.W. (1982). On a possible role of fructose-2,6-bisphosphate in regulating photosynthetic metabolism in leaves. FEBS Lett. **145**, 217–222.

Stitt, M., Cseke, C., and Buchanan, B.B. (1984). Regulation of fructose-2,6-bisphosphate concentration in spinach leaves. Eur. J. Biochem. **143**, 89–93.

Stitt, M., McLilley, R., Gerhardt, R., and Heldt, H.W. (1989). Metabolite levels in specific cells and subcellular compartments of plant leaves. Methods Enzymol. **174**, 518–552.

Taussig, R., and Carlson, M. (1983). Nucleotide sequence of the yeast *suc2 gene for invertase*. Nucl. Acids Res. **11**, 1943–1954.

Turgeon, R. (1989). The sink-source transition in leaves. Annu. Rev. Plant Physiol. Plant Mol. Biol. **40**, 1008–1015.

Vervliet, G., Holsters, M., Teuchy, H., Van Montagu, M., and Schell, J. (1975). Characterization of different plaque-forming and defective temperate phages in *Agrobacterium* strains. J. Gen. Virol. **26**, 33–48.

von Schaewen, A., Stitt, M., Schmidt, R., Sonnewald, U., and Willmitzer, L. (1990). Expression of a yeast-derived invertase in the cell wall of tobacco and *Arabidopsis* plants leads to accumulation of carbohydrate and inhibition of photosynthesis and strongly influences growth and phenotype of transgenic tobacco plants. EMBO J. **9**, 3033–3044.

Weiner, H., Stitt, M., and Heldt, H.W. (1987). Subcellular compartmentation of pyrophosphate and alcaline pyrophosphatase in leaves. Biochem. Biophys. Acta **893**, 13–21.

Yang, N.S., and Russell, D. (1990). Maize sucrose synthase-1 promoter directs phloem cell-specific expression of *Gus* gene in transgenic tobacco plants. Proc. Natl. Acad. Sci. USA **87**, 4144–4148.